Safety Science 79 (2015) 149–162

Contents lists available at ScienceDirect

Safety Science

journal homepage: www.elsevier.com/locate/ssci

Robustness assessment of urban rail transit based on complex network theory: A case study of the Beijing Subway

Yuhao Yang [a], Yongxue Liu [a,b,*], Minxi Zhou [a], Feixue Li [a,b,*], Chao Sun [a]

[a] Department of Geographic Information Science, Nanjing University, Nanjing, Jiangsu Province 210023, PR China
[b] Jiangsu Provincial Key Laboratory of Geographic Information Science and Technology, Nanjing University, Nanjing, Jiangsu Province 210023, PR China

ARTICLE INFO

Article history:
Received 21 October 2014
Received in revised form 4 April 2015
Accepted 9 June 2015
Available online 23 June 2015

Keywords:
Rail transit
Complex network
Robustness
Scale-free
GIS

ABSTRACT

A rail transit network usually represents the core of a city's public transportation system. The overall topological structures and functional features of a public transportation network, therefore, must be fully understood to assist the safety management of rail transit and planning for sustainable development. Based on the complex network theory, this study took the Beijing Subway system (BSS) as an example to assess the robustness of a subway network in face of random failures (RFs) as well as malicious attacks (MAs). Specifically, (1) the topological properties of the rail transit system were quantitatively analyzed by means of a mathematical statistical model; (2) a new weighted composite index was developed and proved to be valid for evaluation of node importance, which could be utilized to position hub stations in a subway network; (3) a simulation analysis was conducted to examine the variations in the network performance as well as the dynamic characteristics of system response in face of different disruptions. The results reveal that the BSS exhibits typical characteristics of a scale-free network, with relatively high survivability and robustness when faced with RFs, whereas error tolerance is relatively low when the hubs undergo MAs. In addition, illustrations of dynamic variations in the influence of the BSS under a series of MAs were provided by spatial analysis techniques of Geographical Information System (GIS), which directly verified the earlier conclusions. We believed the proposed methodology and the results obtained could contribute to a baseline for relevant research of transportation topological robustness.

1. Introduction

Many metropolises such as New York, Beijing, and Moscow have continually increased investments in construction of rail transit lines, resulting in complex subway systems that possess high station densities and intricate inter-station coupling relationships (Angeloudis and Fisk, 2006; Xu and Sui, 2007; Zhang et al., 2012). The applications of such high-capacity subway systems have considerably eased the urban traffic burden caused by the surge of populations. However, the frequent occurrence of random failures (RFs) has increased our awareness of the fact that unreasonable planning as well as insufficient collaborative management measures would impair the overall reliability of a subway system. In addition, malicious attacks (MAs) such as targeted destructions and retaliatory disruptions to the system components can impair the functionality of entire system, causing considerable socio-economic costs (Albert and Barabási, 2002; Lee et al., 2008; Newman et al., 2001; Sparrow, 1991; Wang, 2013; Zhou et al., 2014). Therefore, a better understanding of the topological characteristics of rail transit systems is crucial for improving the robustness of them against both inside disruptions and outside attacks (Crucitti et al., 2003; Derrible and Kennedy, 2010; Kyriakidis et al., 2012; Wu et al., 2008).

The increasing availability of data acquisition on large systems and the rapid development of artificial intelligence techniques aided by computer technology (Vernez and Vuille, 2009; Zhao et al., 2012; Zhong et al., 2010) have led to great advances in our understanding of the topological complexity of critical infrastructures (Ding et al., 2014; Glickman and Erkut, 2007; van der Vlies and van der Heijden, 2013; Zhang et al., 2014). In spite of the significance, the study of these critical infrastructures is an essentially complicated issue since they are continuously growing in complexity and heterogeneity, which makes a single modeling unreliable in this case. As a consequence, multiformalism techniques have been proposed and successfully applied to related works (Flammini et al., 2009b). These techniques have took into account multiple

* Corresponding authors at: Department of Geographic Information Science, Nanjing University, Nanjing, Jiangsu Province 210023, PR China. Tel./fax: +86 25 89681181 (Y. Liu).

E-mail addresses: yangyuhaonju@gmail.com (Y. Yang), yongxue@nju.edu.cn (Y. Liu), zhouminxi_103@hotmail.com (M. Zhou), lifeixue@nju.edu.cn (F. Li), sunchaonju@yeah.net (C. Sun).

http://dx.doi.org/10.1016/j.ssci.2015.06.006
0925-7535/

factors (e.g. occurrence probability of hazard, radiation intensity of hazard, equipment resilience and etc.) related to both intra and internal interactions among different infrastructures, contributing to models that are closer to reality (Bernardi et al., 2011; Sen et al., 2008). Furthermore, recent researches have incorporated quantitative methods to assess the risk of public services, aiming to provide more accurate management plans instead of conventional qualitative ones (Bajcar et al., 2014; Flammini et al., 2009a; Si et al., 2012). Therefore, we are able to conclude that the safety and security investigations in terms of critical infrastructures such as electricity networks, pipelines, and public transportation networks are not an easy issue. Deeper knowledge of the interaction relationships among sub-units in a complex network is thus requisite for an optimization of security system. As a result, _ENREF_16using complex network theory to study the robustness of subway system has become a hot topic in the field of safety management of rail transit systems, given its thorough consideration of the complex interactions relationship in a network. Latora and Marchiori (2002) conducted statistical analyses on the topological properties of the Boston Subway system and concluded that the system exhibited the general characteristics of a small-world network. By comparing 33 metro systems in this world, Derrible and Kennedy (2010) adopted network analysis methods to the transportation literature and offered one application to enhance the robustness of metros. Bruyelle et al. (2014) conducted case studies on the 7/7 London bombings and other subway incidents using common behavioral models and proposed enhancements to the robustness of subway systems.

Admittedly, the size of a subway system is really smaller than a truly complex network. Thus, certain deviations between the features of the Beijing subway system (BSS) and a truly scale-free network are inevitable. However, there are several reasons and advantages for applying complex network theory to investigate the BSS, which consist of the following points: (i) the similarity in evolution pattern. Generally, the evolution of a scale-free network is characterized by a self-organized pattern, which means the new nodes are prone to link to nodes with highest connections in the original network. According to the historical data, the BSS is following a scale-free evolution pattern on the basis of several critical stations (i.e., Xizhi Men station, Xi Dan station, and etc.) (http://en.wikipedia.org/wiki/Beijing_Subway, accessed: September 1, 2014); (ii) conventional applications of complex network to various infrastructures such as power grid networks, internets, pipelines, and aviation networks have proved that the complex network theory, which was summarized from large scale networks, had a potential to be introduced to networks in different scales (Zhang et al., 2012); (iii) incidents occurring to the BSS recent years have demonstrated that when the accidents happened to hub stations, they often resulted in severe dysfunctions and traffic congestions of the subway system. However, these happened to normal nodes generally caused moderate influence on a local region and would be quickly handled (http://en.wikipedia.org/wiki/Beijing_Subway#Accidents, accessed: April 1, 2015). These phenomena in reality implicitly demonstrated the BSS shared similar topological features with a scale-free network. Therefore, three similar attributes between the BSS and a scale-free network, aforementioned, provided us with a premise and strong motivation to explore the BSS from a complex network theory perspective.

Nevertheless, most relevant studies in this field were limited to the field of complex networks, which meant they considered each station as a simple node in graph theory. Few literatures have fully considered the specific circumstances and the inherent topological features of a station. Moreover, the lack of analyses and discussions on geographic elements, economic conditions and population factors would considerably influence the study of configuration and spatial correlation of subway networks, which would be raised up in the current study.

In summary, preliminary identifications of the critical components of network and simulations of the possible scenarios to various accidents are requisite for elevating the resilience of a subway network and for minimizing the aftermath of disruptions. As a consequence, we took advantage of complex network theory in the current study to grasp a sense of the robustness of the BSS, aiming to identify the generic topological features of the transit networks. Moreover, spatial analysis techniques of Geographical Information System (GIS) were applied to conduct quantitative analyses on the spatial influence of the large subway system.

2. Background

2.1. The Beijing Subway system

Beijing, the capital of China, is the nation's political, economic and cultural center with a total area of 16,410 km^2 and a registered population more than 21 million. Until May, 2014, the BSS has a total of 18 lines, 279 stations, 41 transfer stations and a mileage more than 544 km (Fig. 1), ranking it the second largest subway to Shanghai in the world (http://en.wikipedia.org/wiki/Beijing_Subway, accessed: September 1, 2014). The BSS supports the majority public transit of Beijing City (over 3.6 billion rides in 2013), making it the busiest subway system in the world. All these features make it an ideal sample to investigate the robustness of the subway transit system. Stations and lines data (including those under construction) were acquired from the Beijing Subway official website (http://www.bjsubway.com/, accessed: December 23, 2013). All data were first geo-referenced to WGS-84 coordinate system to ensure the accuracy of data registration.

2.2. The definition of various failures and attacks

A subway network system generally encounters two types of incidents, i.e., random failure (RF) and malicious attack (MA) (Kyriakidis et al., 2012; Wang et al., 2014; Wang, 2013). Common behaviors of these two were summarized to Table 1.

The occurrence of subway accidents can be attributed to a great many precursors, varying from a natural error to an anthropogenic attack (Lu et al., 2013; Wang and Fang, 2014). Due to the uncertainties of these precursors, it is extremely difficult to quantitatively specify the corresponding destructive power for each failure or attack. As a consequence, we specified a RF as the dysfunction of a network caused by failure on one or several nodes with a random probability, whereas a MA as a targeted destruction manipulated by outside artificial forces (Ghedini and Ribeiro, 2011; Zhang et al., 2012). The difference of these two scenarios involves two aspects: (1) the probability of a RF is equal among all stations while MAs generally happen to hub stations with high degree or centrality; (2) the destructive power of a random anomaly is insignificant compared with a MA that would degenerate the function of entire station or line for a long time.

It should be noted that natural disasters were not taken into account in the study because we fundamentally assumed that natural disasters, which were able to impact the underground subway network, generally meant devastating destruction on a whole transportation system. For instance, the 2011 floods in Southeast Queensland destroyed the whole transportation system, which could hardly be simulated by a few stations or lines. However, these natural factors would play an important role in the safety assessment of large-scale transportation system, such as shipping and aviation that are exposed to external circumstances frequently.

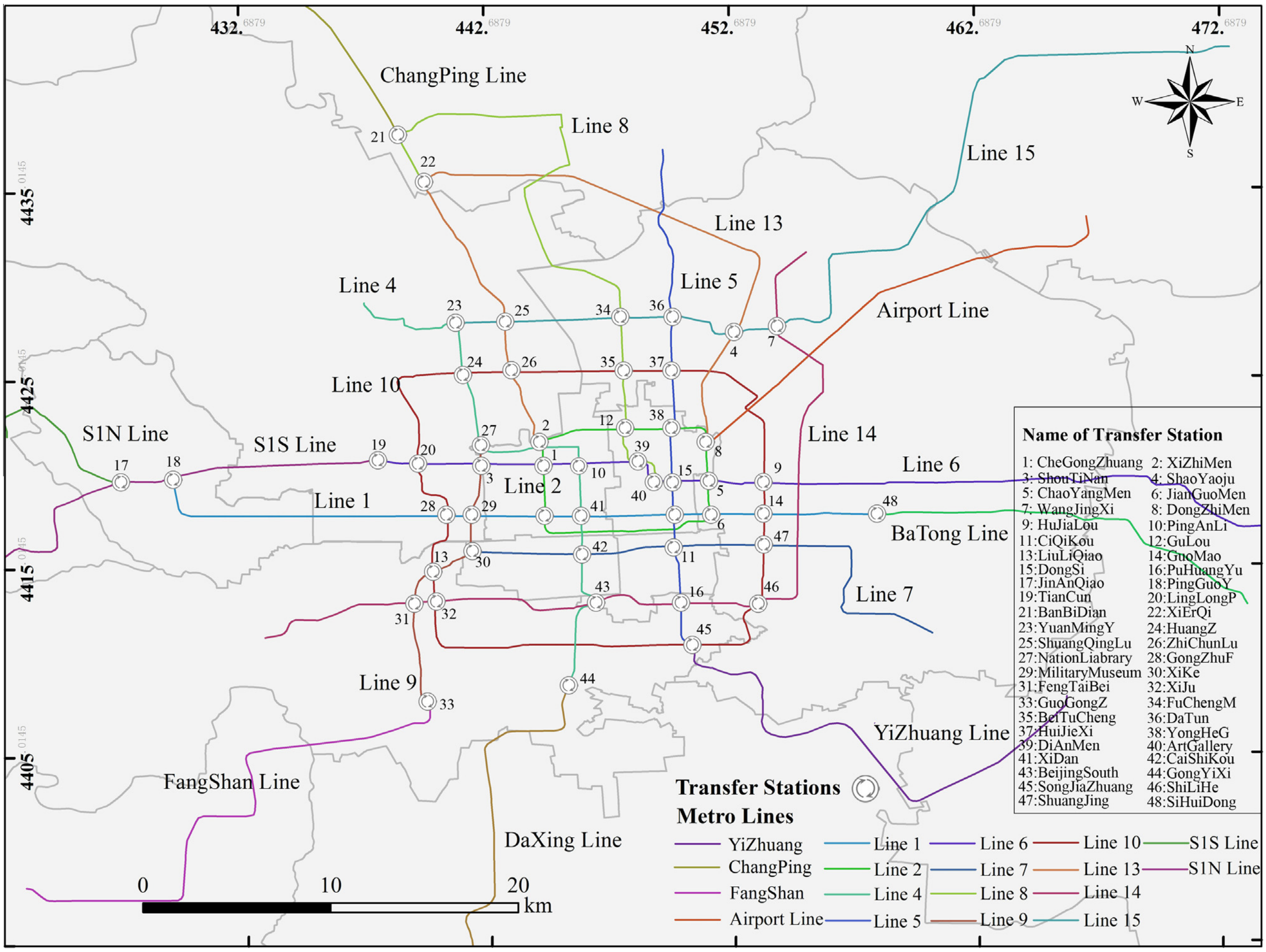

Fig. 1. Schematic map of the BSS structure.

Table 1
Summary of common behaviors of failures and attacks for a subway system.

Categories	Precursors	Description
Random failure	Technical malfunctions	Broken rail, Broken wheels, Brake failure, Gear Failure, Signal failures, Power failure, Crack rail, Line fault, Exceeding speed
	Passengers actions	Congestion, Suicide in platform, Fall onto track, Falls on escalators, Group fighting, Unconscious destruction due to drunkenness, Smoke in station/train, Wrong operation by driver, Passenger carrying dangerous goods, Passenger carrying pets, Riot caused by rumors, Caught in train doors
	Official actions	Temporary disruption of service, Temporary line maintenance, Temporary closure for safety inspection, Temporary closure for special activity, Decision error
Malicious attacks	Targeted destruction	Deliberate destruction, Passenger carrying dangerous/flammable goods, Passenger carrying poisonous goods, Kidnapping, Trespass, Manual destruction on rail, Manual destruction on train, Explosion in purpose, Set fires, Gun shooting, Derailment caused by human, Deliberate assassination to raise riot and etc.

2.3. Fundamental concepts of network performance

Survivability, or robustness of a rail transit network, is determined with respect to different accidental behaviors. The fundamental definition of network survivability, also called resilience, is that a network is able to maintain its partial characteristics in face of disruptions to its network components (Murray et al., 2008). Robustness in this field deals more particularly with the ability of a subway system to provide alternative routes when accommodating variations in traffic demand. Fundamental concepts such as reliability, vulnerability and tolerance are essential to be specified, which are applied to assess the fault tolerance of a local station as well as a global network (Berche et al., 2009). Hereinafter, we took the terms of failure tolerance to represent the robustness of a subway network when confronting RFs. The notion of attack vulnerability denoted the survivability of a metro network under MAs (Albert et al., 2000; Derrible and Kennedy, 2010; Wang, 2013; Zhang et al., 2012).

3. Methodology

The research work consists of the five aspects (Fig. 2): (i) a calculation of the topological properties of the BSS to identify which network category it may belong to; (ii) a combination of two centralities to generate a new index to position hub stations; (iii)

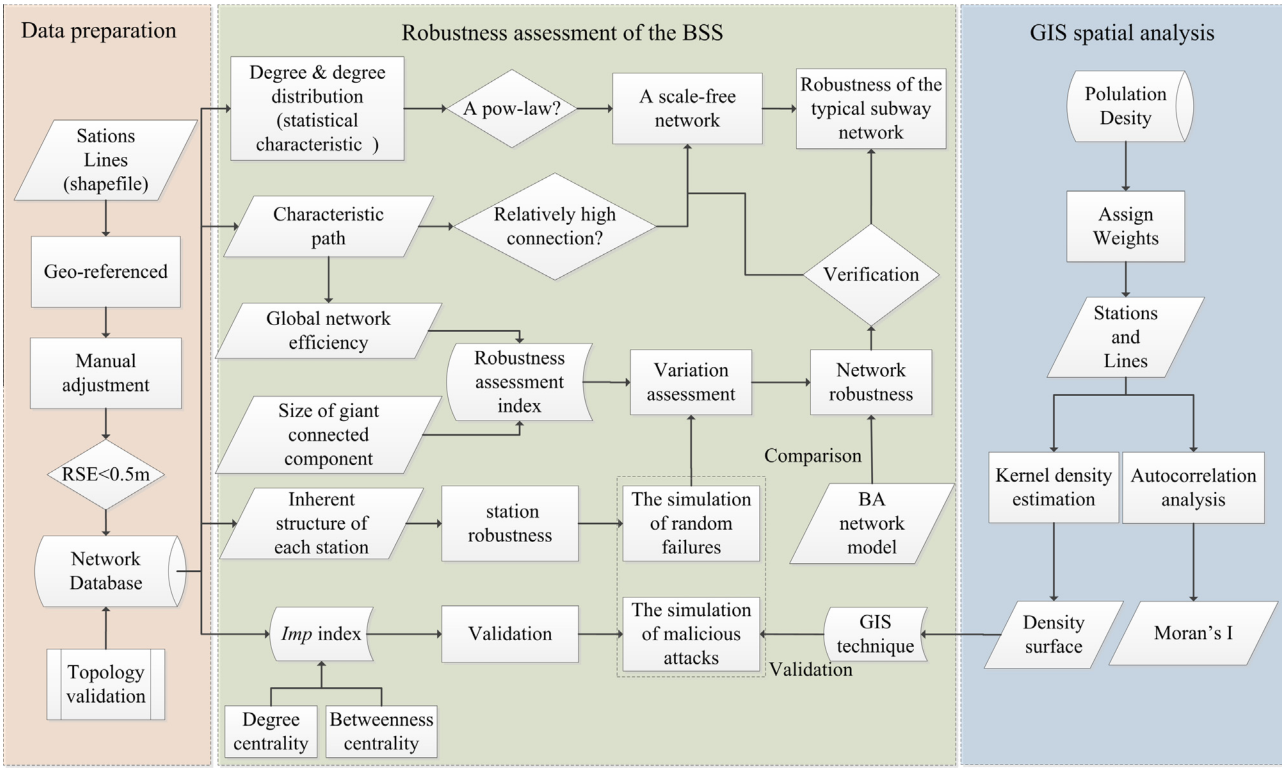

Fig. 2. Flow diagram for robustness assessment of the BSS.

quantitative comparisons between the BSS and a statistical ensemble to verify the former judgment in the first step; (iv) a GIS technique as an auxiliary strategy to validate the analysis of topological robustness from a spatial correlation perspective.

3.1. Topological properties of the BSS

3.1.1. Degree and degree distribution

In the context of subway network research, the k_i refers to the number of lines connected to station i, and it represents the local property of station i. Degree distribution P_k is the probability of a node with degree k, which is a probability distribution function over the whole nodes (Bruyelle et al., 2014; Strogatz, 2001). In a complex network model, there is a statistical correlation between degree and its distribution (Kim and Wilhelm, 2008). Substantial empirical and theoretical results reveal that the topological characteristics of many real networks are reproduced by the scale-free model (Albert and Barabási, 2002; Wu et al., 2008), which means the node degree k and degree distribution $P(k)$ in the network satisfy a power-law distribution Eq. (1).

$$P(k) \sim k^{-\gamma} \tag{1}$$

where y is the scale factor which generally ranges from 2.10 to 5.52 in most metros (Derrible and Kennedy, 2010). In addition, a typical property of the scale-free network is that most nodes contain small degrees, whereas a few nodes (also known as "hubs") have high connectivity (Clauset et al., 2009; Zhou et al., 2014). Whether the BSS belongs to a scale-free one is a key issue for identification of the topological complexity and structuring mechanism of the BSS prior to further analyses.

3.1.2. Average path length

Average path length, also known as characteristic path length, is defined as the average number of steps along the shortest paths for all possible pairs of network nodes (Nawrath, 2006). This value directly indicates the overall connectivity as well as the size of a network. Moreover, it is an essential part in the construction of robustness indicators which are applied to evaluate the error tolerance and attack vulnerability of a network. Therefore, in the current research, the shortest distance d_{ij} between two random stations i and j was first calculated using the breadth-first search (BFS) algorithm (Tarjan, 1972), a safe searching strategy regardless of potential disconnections. The average path length D was then calculated by Eq. (2).

$$D = \frac{1}{N(N-1)} \sum_{i \neq j} d_{ij} \tag{2}$$

3.2. Node importance evaluation based on weighted degree and betweenness

In a complex transportation system, not all stations are equivalent. Prior to the evaluation of the survivability of a network, a crucial step is to position the hubs. Conventional researches usually regarded the degree centrality of a node as the only measurement for evaluating the significance of the node. However, an inspection of degree centrality revealed that it was not reasonable to use such a local quantity to evaluate the whole function of a node without considering its global effect (Barthélemy, 2004). As a result, betweenness (Eq. (3)), which counts the fraction of shortest paths passing through a given node, has been proposed and used as a global geometric factor for node importance evaluation (Benton and Fernández Fernández, 2013; Brandes, 2008; Crucitti et al., 2003; Ghedini and Ribeiro, 2011; Wang et al., 2014).

$$b_{k \in G} = \sum_{i \neq j} \frac{m_{ij}(k)}{m_{ij}} \tag{3}$$

where m_{ij} is the number of all shortest paths, and $m_{ij}(k)$ is the number of shortest paths passing through node k in a graph G.

According to Abbasi et al. (2012), betweenness is an effective measurement of the global function of a node compared to degree. A node with high betweenness usually plays a critical role in maintaining effective communication among various nodes in a network. However, betweenness alone is not able to effectively measure the local clustering performance of a node as degree centrality.

To sum up, it seems that for a complex network comprised by great many clusters and loops, the local properties, i.e., degree centrality, can better represent the function of a node. With the increasing number of the global connections, a node playing the role of the bridge among various important components tends to be more powerful. Malfunctions on these nodes will considerably affect the connectivity of a network (Wang et al., 2011). Therefore, we fundamentally supposed a combination of degree and betweenness was able to explicitly evaluate the function of a node from both local and global scope. A new node importance evaluation index (*Imp*) based on the weighted sum of the two indicators was, therefore, presented in this study to assess node importance in a real network (Eq. (4)).

$$Imp_{i\in G} = n_1 b_{i\in G} + n_2 D_{i\in G} \tag{4}$$

where $b_{i\in G}$ is the betweenness of node i, $D_{i\in G}$ is the degree of node i, and n_1 and n_2 are the corresponding normalized weighed coefficients. In this study, the values of the two coefficients were set to be 0.6 and 0.4.

Considering the different values of n_1 and n_2 would influence the performance of *Imp* when applied to different complex networks. Thus choosing appropriate values for these two coefficients is a key issue when constructing a new index to assess node importance (see Section 5.2).

3.3. Robustness assessment model of subway stations

Relevant studies aforementioned generally regarded a transfer station as a simple spatial point. Based on their assumption, all lines connected to this point would be out of order simultaneously when encountering an accident. However, the intrinsic robustness of the internal structures of a transfer station was ignored, which might result in considerable errors. For instance, different lines might converge to different transfer sites/joints in a large transfer station (Fig. 3). Given that a MA usually results in severe damage and is able to destroy a whole station, the aforementioned assumption can be justified. However, the inference may not be valid in terms of a RF which is unlikely to cause widespread and cascading disasters.

Consequently, stations containing multiple transfer sites for different lines were first selected in order to evaluate their inherent robustness prior to a comprehensive analysis on the robustness of a global network. Subsequently, the linear distance L_i between two transfer sites within station i was calculated (Fig. 3a), which was then used to measure the size of a station. For stations involving three transfer sites, the corresponding radius R_i of the circumscribed circle was calculated according to Eq. (5), which was then multiplied by the number of transfer sites n to obtain the corresponding distance L_i in station i (Fig. 3b). The circumscribed circle method here is also applied to stations with more than three transfer sites.

$$R_i = \frac{abc}{\sqrt{[(a^2+b^2+c^2)^2 - 2(a^4+b^4+c^4)]}} \tag{5}$$

where a, b and c represent the length of each side for a triangle, respectively, and i is the label of a station which contains multiple transfer sites.

The maximum distance L_{Max} was subsequently able to be obtained by a sorting searching in the distance set. Based on the core idea of the inverse-distance weighting method, the closer different transfer sites are in distance, the more related them are. Subsequently, the L_{Max} and L_i were applied to calculate the dysfunction probability P_i of station i under a RF (Eq. (6)).

$$P_i = (1 - L_i/L_{Max}) * 100 \tag{6}$$

where L_i is the aggregation of all distances among various transfer sites in a station, and L_{Max} is the maximum one in the distance set. Afterwards, the radio between L_i and L_{Max} was calculated and then was subtracted by 1 to reverse its value, which is set to the final dysfunction probability P_i of station i.

It should be noted the destructive power of a RF is generally small. Therefore, for a practical subway network, the transfer sites are usually supposed to have few mutual impact on each other (i.e., $P_i = 0$) when the distance between them is greater than 500 m. Therefore, the disruption probability P_i' of line i during a RF was calculated according to Eq. (7), where n is the number of lines in the station i. For a regular station or a transfer station without any transfer site, both P_i and P_i' were set to 100%. In the subsequent simulation on the robustness of the BSS, an evaluation of the global error tolerance of a network was conducted based on P_i and P_i'.

$$P_i' = (P_i/n) * 100 \tag{7}$$

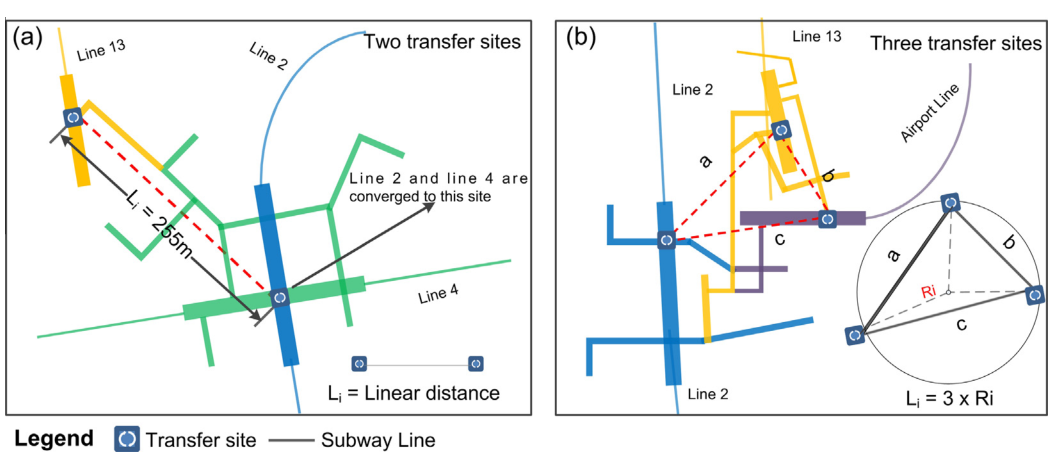

Fig. 3. (a) Schematic map of the Beijing Dongzhimen subway station structure; and (b) schematic map of the Beijing Xizhimen subway station structure. In the former station, there are only two transfer sites. Thus, the distance L_i is equal to the Euclidean distance between these two transfer sits. However, in the latter scenario, L_i is the three times of the radius of the circumscribed circle.

3.4. Robustness assessment model overall performance of a network

The efficiency and performance of a network generally rely on its topological completeness in terms of several hub nodes and lines. Several models have been proposed to provide insights to the structural characteristics of a network (Queiros-Conde et al., 2007; Queiros-Conde, 2003). In the current study, an evaluation model to assess the global performance of a network under various attacks was established based on two indicators, i.e., relative size of the maximal connected sub-graph (*RSMCS*) and global network efficiency (*GNE*), both of which are widely used in the field of complex network analysis (Berche et al., 2009; Crucitti et al., 2003; Ghedini and Ribeiro, 2011). The measurement of *GNE* is performed by computing possible shortest distance between any two nodes in the network, which represents the information of network in global scope. Meanwhile, the measurement of *RSMCS* is based on the size of the giant component, which focuses on local characteristics of a specific component. Therefore, we combined these two indexes to explore how the topological properties of the BSS responded to different accidents from both global and local scopes.

3.4.1. Assessment model for overall performance of a network based on RSMCS

If any two vertices in a graph are connected, the graph (G) is called a connected graph. When nodes are under attack, the entire connected graph will be divided into multiple sub-graphs. The one having most connected nodes is known as the maximal connected sub-graph (Fig. 4). *RSMCS* here is defined as the ratio between the number of nodes N_{max} in the maximal connected sub-graph and the number of nodes N in the initial network (Eq. (8)).

$$S = N_{\max}/N \tag{8}$$

3.4.2. Assessment model for overall performance of a network based on GNE

The characteristic path length represents the efficiency of a network, and these two are negatively correlated to each one. However, when nodes in a network are under attack, the shortest path length of two unconnected nodes stored in an adjacent matrix is infinite (∞). As a result, the characteristic path length cannot be computed. At this time, the reciprocal of the distance $d_{i,j}$ between nodes i and j (i.e., $e_{i,j} = 1/d_{i,j}$) is 0. Therefore, the *GNE* (E_G) of the network is calculated through Eq. (9).

$$E_G = \frac{1}{N(N-1)} \sum_{i \neq j \in G} \frac{1}{d_{i,j}} \tag{9}$$

Table 2
Population densities and areas of sixteen districts in Beijing (2010). Relevant data can be inspected at http://en.wikipedia.org/wiki/Beijing, accessed: September 1, 2014.

District/County	Population	Area (km^2)	Population density (per km^2)
DongCheng	919,000	40.6	22,635
XiCheng	1,243,000	46.5	26,731
ChaoYang	3,545,000	470.8	7530
FengTai	2,112,000	304.2	6943
ShiJingShan	616,000	89.8	6860
HaiDian	3,28100	426.0	7702
MenTouGou	290,000	1331.3	218
FangShan	945,000	1866.7	506
TongZhou	1,184,000	870.0	1361
ShunYi	877,000	980.0	895
ChangPing	1,661,000	1430.0	1162
DaXing	1,365,000	1012.0	1349
HuaiRou	373,000	2557.3	146
PingGu	416,000	1075.0	387
MiYun	468,000	2335.6	200
YanQing	317,000	1980.0	160

3.5. A validation strategy using GIS technique

3.5.1. Kernel density analysis based on population density

After each MA, a certain number of stations and lines would be destroyed and the influence of the BSS would be decreased continuously. For a specific station, its daily ridership would be positively related to the population density around it, i.e., the greater population there is in a district, the greater need there is for subway transportations. Therefore we utilized the population data (Table 2) as weighting factors to evaluate the influence of the BSS by means of a density analysis, which aims to provide insights to how the influence of the BSS varies under MAs.

Specifically, the process consisted of three fundamental steps: (1) different weights, i.e., population densities of different districts, were assigned to stations and lines according to their locations (Fig. 5b) through an overlay analysis in ArcGIS (http://www.esri.com); (2) the influence of each station and line was then able to be quantitatively evaluated using a kernel density analysis in ArcGIS according to the weights assigned to them. Based on a kernel function (Eq. (10)), this density analysis was designed to calculate magnitude per unit area to fit continuous surface to point and polyline features; (3) the density surfaces of points D_{point} and polylines $D_{polyline}$ were integrated to generate a smooth surface *Influence*(i, j), which represented the global influence of the BSS (Eq. (11)). Finally, a standardized *Influence*′ (i, j) was obtained to eliminate the distribution divergence of elements in Eq. (12).

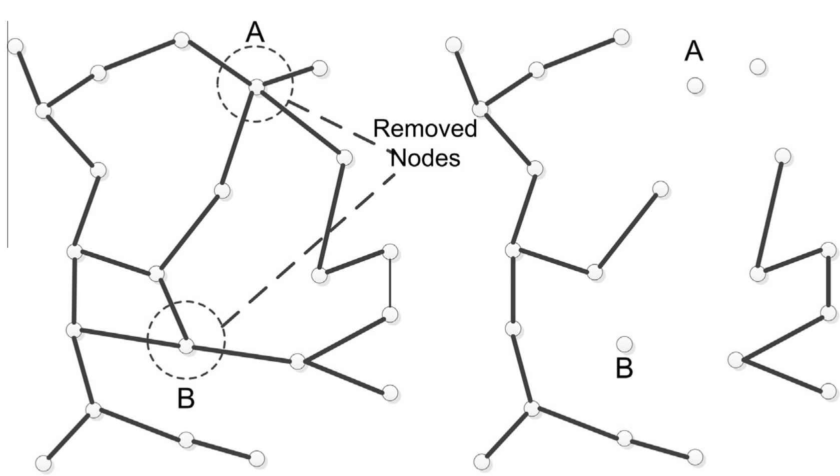

Fig. 4. Structures of the connected graph before and after node removal.

$$f(x|h) = \frac{\sum_{i=1}^{n} k_h(x - x_i)}{n} \tag{10}$$

where $x_1,\ldots, x_n$ is an independent and identically distributed observations derived from an unknown probability density $f(x)$. The attempt of this estimation is to draw the shape of the function $f(x)$. k_h is a kernel function. h is the bandwidth which controls the scale of the kernel function, often defined as $k_h = \frac{1}{h}k(x/h)$ (Silverman, 1986).

$$Influence(i,j) = D(i,j)_{point} + D(i,j)_{polyline} \tag{11}$$

where i, j is the row and column of a raster surface, and $Influence(i,j)$ represents the power of the BSS posed on different districts.

$$Influence'(i,j) = \frac{Influence(i,j)}{\sum_{j=1}^{n} Influence(i,j)} \tag{12}$$

3.5.2. Spatial autocorrelation analysis

Due to the dense distribution of a subway network, it is reasonable to infer there would be specific relationships in geographical space between neighboring stations. The dysfunction of specific stations under continuous MAs would result in damage on global autocorrelation for the entire subway network. Therefore, we adopted the global Moran's I (Eq. (13)), a common and important measurement of spatial autocorrelation (Cliff and Ord, 1981; Moran, 1950), to evaluate the spatial autocorrelation feature of the BSS and its variation patterns under MAs, aiming to identify the relationship between the spatial distribution patterns and the influence of the BSS. Similar to the aforementioned analysis, corresponding population densities were taken as the weights in this spatial analysis.

$$I = \frac{n}{S_0} \cdot \frac{\sum_i^n \sum_{j=1}^n w_{ij}(x_i - \bar{x})(x_j - \bar{x})}{\sum_i^n (x_i - \bar{x})^2} \tag{13}$$

where x_i represents the population density around station i, the value w_{ij} is the weight assigned to station i and j, which represents the topological relationship between spatial units, i.e., 1 means adjacent and 0 otherwise. S_0 is the sum of all the elements from w_{ij} and $\bar{x} = \frac{1}{n}\sum_{i=1}^{n} x_i$ is the average of the population densities in all stations.

4. Results

4.1. Topological characteristics of the BSS

4.1.1. Degree and degree distribution: a scale-free network

Statistic results show that approximately 80% nodes in the BSS have a degree of two (Fig. 6a) (detail is shown in Appendix Table A1), suggesting that the expansion of a regular rail transit network follows a mode of linear expansion. Subsequently, a least-square method was used to fit the double logarithmic of node degrees and of degree distribution, resulting in: $p(k) = 26.11k^{-5.07}$, indicating the degree distribution of the BSS conforms to a power-law distribution of $\gamma = 5.07$ to a certain extent.

4.1.2. Characteristic path length: relatively high connectivity

The shortest distances between stations in the BSS and corresponding frequency of each distance were shown in Fig. 6b. Results show averages of 15 stops are required for each Beijing resident to reach destination when riding the subway. As the average time span between two stations in Beijing Subway is about 2 min, passengers are often able to arrive at their destinations in 30 min, which really means a fast transportation in a metropolis.

4.1.3. Positioning Hubs based on Imp

The node importance index (*Imp*) of each station in the BSS was first calculated according to Eq. (4), and 42 stations with high *Imp* were selected. Specific details of them were listed in Table 3. The validation and effectiveness of the *Imp* were discussed in Section 5.1.

4.2. Station robustness of the BSS

For the evaluation of robustness of subway stations, RFs were performed on each station, followed by topology reconfiguration of the network according to the failure probability of each station and line. Simultaneously, variations in the *GNE* and *RSMCS* of the network were compared with those recorded without considering

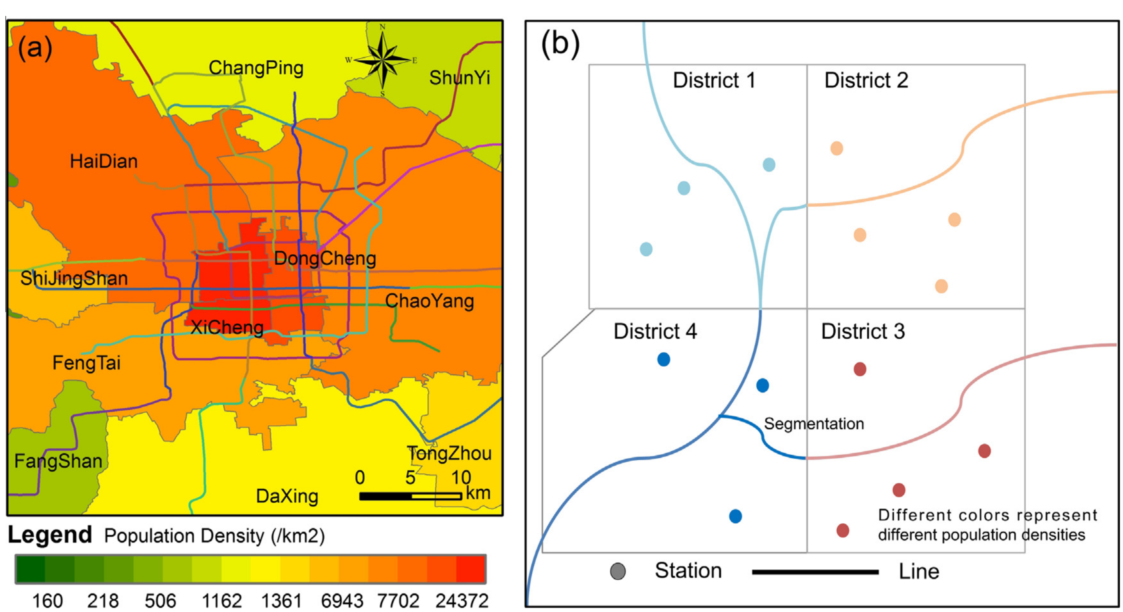

Fig. 5. (a) Distribution of the population density in eleven basic districts. (b) The conceptual diagram of the weight assignment process. Line segments and stations are overlaid by the district polygons, and the population density of each district is assigned to features that located in its coverage.

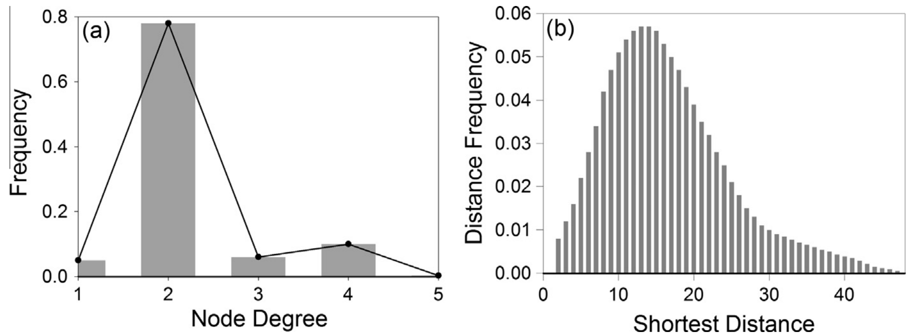

Fig. 6. (a) Degree distribution of the BSS. (b) Frequency distribution of the shortest inter-station distance in the BSS.

Table 3
Details of the hub stations in the BSS; type 0 means a regular station; 1 means a transfer station with different transfer sites; 2 means a station under construction; 3 means transfer stations without different transfer sites and D, P_i, and P_i' of these stations were set to, 0%, 100%, and 100%, respectively.

Name	Type	*Imp*	D (m)	P_i (%)	P_i' (%)	Name	Type	*Imp*	D (m)	P_i (%)	P_i' (%)
CheGongZhuang	1	1.00	145	71.0	35.5	FengTai	2	0.52	0	100	100
XiZhiMen	1	0.95	225	49.0	24.5	FuXingMen	1	0.51	112	78.0	39.0%
ShouTiNan	2	0.86	0	100	100	CaiShiKou	3	0.50	0	100	100
ShaoYaoJu	1	0.69	161	68.0	34.0	JiaoMenXi	3	0.50	0	100	100
ChaoYangMen	1	0.68	0	100	100	LingLong	2	0.50	0	100	100
JianGuoMen	1	0.68	135	75.0	41.0	XiKe	2	0.50	0	100	100
WangJingXi	1	0.64	350	21.0	6.3	LongFuShi	2	0.49	0	100	100
BaiLiQiao	1	0.62	60	88.0	44.0	ZhiChunLu	1	0.49	170	66.0	33.0
HuJiaLou	3	0.62	0	100	100	XuanWuMen	3	0.47	0	100	100
PingAnLi	1	0.62	160	68.0	34.0	JiShuiTan	0	0.46	0	100	100
CiQiKou	3	0.59	0	100	100	NanLuoGu	1	0.46	75	85.0	42.5
GuLouStreet	1	0.59	145	71.0	35.5	BeiTuCheng	3	0.45	0	100	100
LiuLiQiao	2	0.59	0	100	100	CiShouShi	1	0.39	115	77.0	38.5
GuoMao	1	0.58	152	70.0	35.0	QiLiZhuang	1	0.34	100	80.0	40.0
JinTaiLu	2	0.56	0	100	100	XiJu	1	0.34	65	87.0	43.5
DongSi	1	0.54	94	81.0	40.5	XiDan	1	0.32	245	51.0	25.5
PuHuangYu	2	0.54	0	100	100	LiShui	0	0.29	90	82.0	41.0
ZhanLanLu	2	0.53	0	100	100	YongHeGong	1	0.26	105	79.0	39.5
CongWenMen	1	0.52	133	74.0	37.0	SanYuanQiao	1	0.24	105	79.0	39.5
DiAnMen	2	0.52	0	100	100	HuoYin	1	0.15	156	69.0	34.5
DongZhiMen	1	0.52	504	0.0	0.0	MilitaryMuseum	0	0.15	190	62.0	31.0

the internal structures of the stations. As is illustrated in Fig. 7, when faced with RFs in identical destructive power, two network performance indicators for the network considering inherent robustness of stations are generally higher than their adversary, which means better survivability. As a result, we can infer that the structural feature of a subway station is an essential element in robustness assessment study.

4.3. Variations in the network performance of the BSS

According to the obtained results (Section 4.1), the degree distribution of the Beijing subway network approximately follows a power-law tail. Therefore, a scale-free network model, Barabasi Albert (BA) network, in same scale was constructed as a cross-validation to ensure the generic application of our analysis. In terms of RFs, nodes in the BA network were iteratively and randomly removed in the same proportions. Changes in the network's performance were compared to those of the real network which incorporated the inherent robustness of each station. As for MAs, 30 hubs in the real network (approximately 10% of the total nodes) were selected based on the analysis results presented in Section 3.1. These nodes were then iteratively removed to analyze the variations in efficiency of the BSS under MAs. Meanwhile, nodes in the BA network were removed in a same way for a reference.

Results in Fig. 8a reveal the variations of the *GNE* (E) under different attacks. When 10% of the nodes were destroyed under RFs,

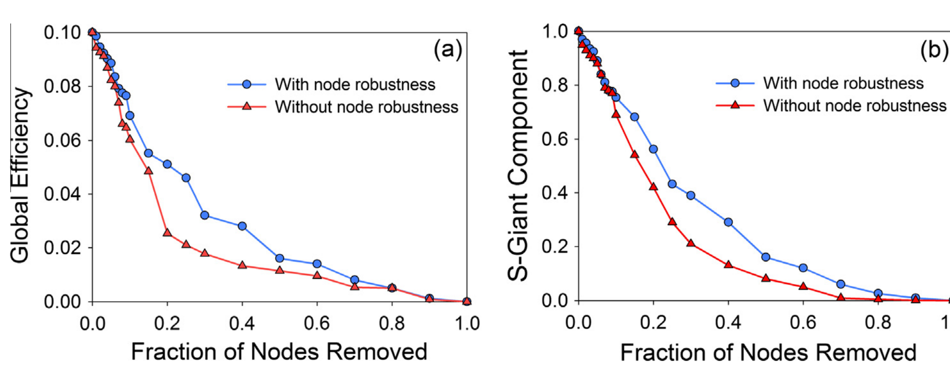

Fig. 7. Variations in real network's *GNE* and *RSMCS* in a RF scenario; when (a) considering, and (b) without considering the inherent robustness of a station.

the value of the *GNE* decreased slightly in both networks. The range of decrease was from the initial value of 0.1 to a value greater than 0.07. In the case of MA with targeted destruction of nodes, *E* decreased instantly from 0.1 to less than 0.02. Therefore, the range of decline under MAs is much greater than that observed during RFs.

The variation patterns of *RSMCS* in the two networks are generally consistent with *GNE* (Fig. 8b). When the network underwent a minimal fragmentation ($f < 0.1$), the value of S showed an insignificant difference compared to the size of original network under a RF, whereas the value already decreased to 0.8 under a MA. With continual destructions, the network almost collapsed under a MA when 10% of the nodes were removed. However, under RF, the S value decreased only to 0.7 of the initial value, maintaining relative stability.

Afterwards, two regression analyses were carried out to study the relationship between the BSS and the BA network. As is depicted in Fig. 8e and f, the variation trend of the BSS shows good agreement with the BA network in terms of *RSMCS*, and the coefficients of determination (R^2) of linear regressions are 0.948 and 0.979, respectively. As for the *GNE*, the regression results show that there is also a strong correlation between the BSS and the BA ($R^2 = 0.922$ and 0.876, respectively). Two regression results together reveal that the topological robustness of BSS is similar to a scale-free network in terms of both local and global scope.

4.4. Results derived from two GIS analysis strategy

4.4.1. Variations in network influence caused by MAs

A visual inspection shows that the influence of the BSS radially decreases in every direction under MAs (Fig. 9). With the continuous destructions happening to the central hub nodes of the subway network, the size of areas highly impacted by the subway (red zone) decreases rapidly, indicating the decline of the subway influence. When all these hub nodes were damaged to some extent, there was hardly a region significantly influenced by the BSS. This trend indirectly indicates the accessibility to urban rail transit system will change dramatically if the hubs are destroyed, which enhances our awareness that correct strategies to protect and plan the critical stations reasonably are essential for transportation safety. Furthermore, these illustrations (Fig. 9) verify the predictions and analyses of the variations in the network performance of the BSS under MAs (Section 4.2).

4.4.2. Variations in autocorrelation caused by MAs

The variations in global efficiency of the BSS under iterative MAs are presented in the Fig. 10, combining with changes in spatial autocorrelation measured by Moran's I. A visual inspection reveals that the global correlation of the BSS is related to the completeness of the subway structure. As is discussed in Section 3.5, the spatial autocorrelation of stations means the survivability of a subway

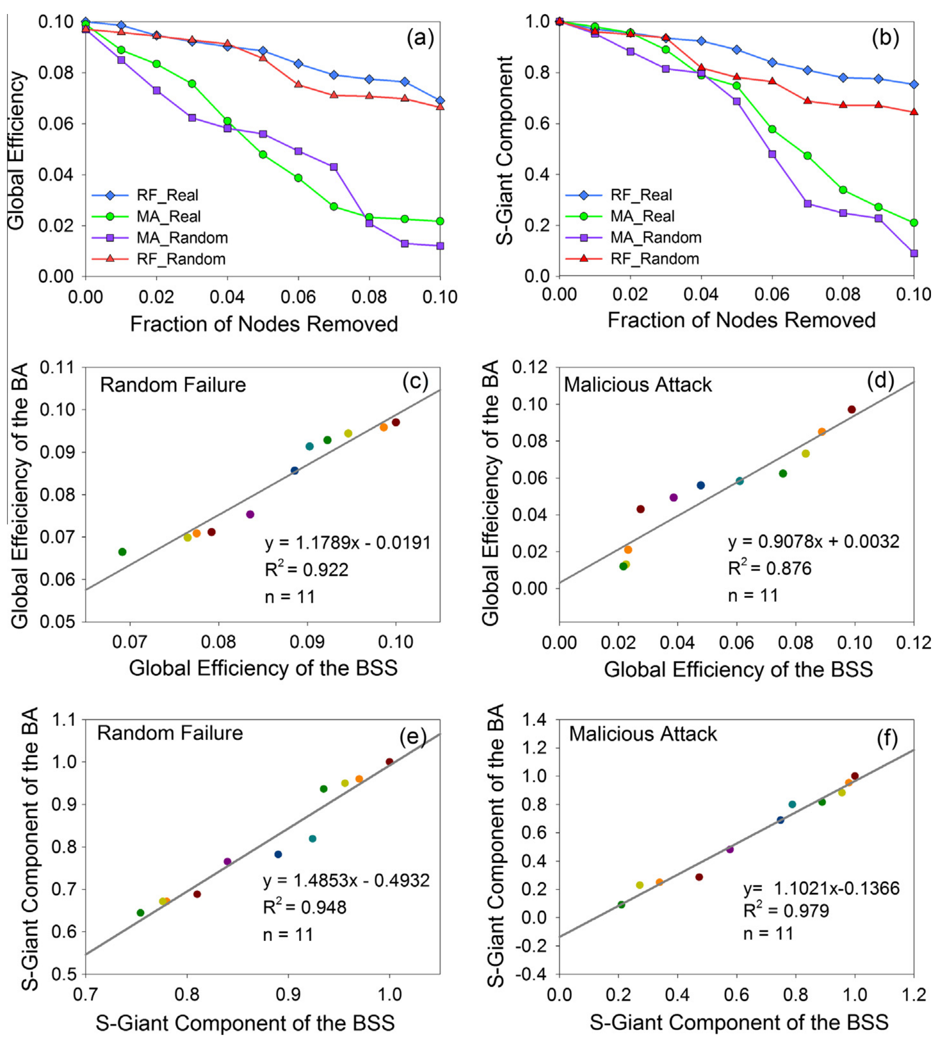

Fig. 8. Variations in (a) *RSMCS* and (b) *GNE* in four scenarios: RF on a real network (RF_Real), MA on a real network (MA_Real), MA on a random network (MA_Random) and RF on a random network (RF_Random). (c)–(f) are four regression analyses to provide insights to the relationship between the BSS and the BA network derived from the variation trends in (a) and (b).

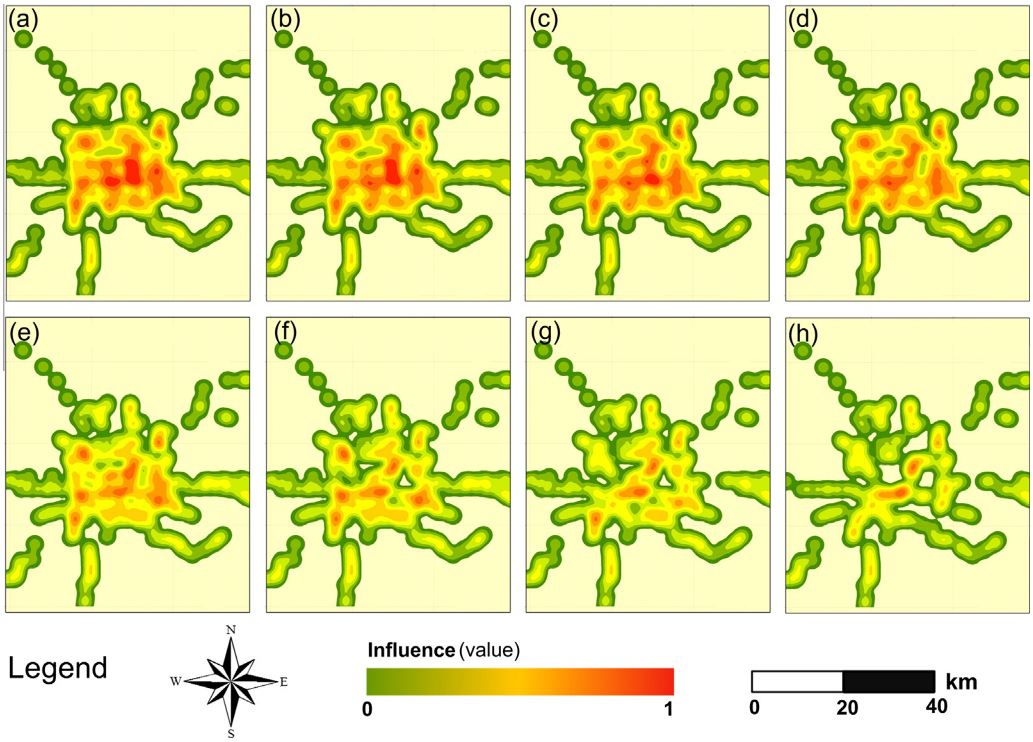

Fig. 9. Variations in the power distribution of the BSS under MAs (an iterative process that removes 2% hub nodes in each iteration).

system when taking the population density as the influence weights. Thus, this result is able to validate the variation tendency of global efficiency measured by *GNE*. A linear regression shows the correlation between global correlation and network efficiency is strong ($R^2 = 0.9487$). This phenomenon is attributed to the particular distribution of hub stations and population density in Beijing, which will be further discussed in Section 5.3.

5. Discussions

5.1. Validation and significance of the Imp

Results in Fig. 8 shows dysfunction in hub stations can cause severer damage to a rail transit than normal ones. Therefore, it is essential to accurately position hub stations when relevant administrations need to improve the overall robustness of a specific rail transit system. As is mentioned in Section 3.2, betweenness indicates the function of nodes in the entire network, and dysfunction can therefore occur on the whole network as the nodes with high betweenness are attacked. Thus, targeted attacks were performed on the real network based on the sorted results of node *Imp*, betweeness and degree in the current study, respectively. Variations in *RSMCS* and *GNE* of the network (Fig. 11) under different attack scenarios were compared in order to validate the *Imp*.

As is demonstrated in the Fig. 11, under same scale attacks, the values of both indicators obtained based on *Imp* are less than those obtained based on degree or betweenness alone when the fraction of nodes removed from the real network is in the range of 0.0–0.06.

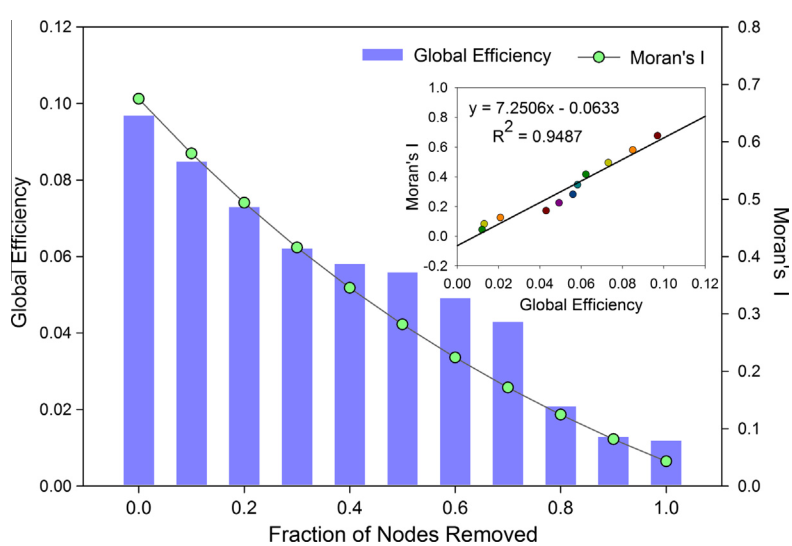

Fig. 10. The relationship between the global efficiency of the BSS and the global Moran's I of the population density in Beijing. The result of a regression analysis is also shown inside.

This variation tendency means that dysfunction of nodes with high *Imp* causes more severe damage to the network. As the fraction of nodes removed exceeds 0.06, the network is divided into various sub networks and the severity of destruction gradually stabilized. Consequently, the results described above are able to verify the effectiveness of *Imp* proposed in this work. Hub stations of the BSS are able to be accurately positioned according to this criterion.

5.2. Parameters tuning

What deserves to be mentioned is that in Section 3.2 there are two corresponding weighed coefficients (Eq. (4)), i.e., n_1 and n_2, which control the specific value of *Imp*. In our experimental process, we set n_1 and n_2 to five set of values, i.e., 0.6 and 0.4, 0.4 and 0.6, 0.8 and 0.2, 0.2 and 0.8, 0.5 and 0.5 respectively. By comparing the results (Table 4) derived from analyzing the variations in the network performance, an optimum set value, i.e., 0.6 and 0.4 was finally obtained for the two weighed coefficients. The difference among several parameters set is determined by the topological structure of the BSS. To be specific, the betweenness is a global measurement of the function in terms of a single node while the degree is a strategy used to evaluate the ability of a node to maintain connectivity in a local component. Therefore, we can infer that *Imp* with a high weighting value of betweenness is appropriate for a subway network that consists of intricate connections, e.g., Tokyo Subway, which is abundant in stations acting as the global bridges between various sub-regions. On the contrary, *Imp* in high degree centrality would be suitable for subway system full of local clusters, such as the Seoul Subway and the New York City Subway.

Due to the limited number of stations in the BSS, the difference between each *Imp* was subtle. But we inferred that with the expansion of the scale of urban rail transit systems, the divergence between local property and global performance would become more remarkable.

5.3. Robustness of subway to failure and attack

Since the development of the modern society is severely affected by the self-organized transit networks (Zhang et al., 2012), robustness of a subway operation should be paid more attention. In other words, the planning of topological structure is a critical issue of great operational significance for subway system. In the current study, we have contributed to exploring the topological features and sensitivity of the BSS to failures and targeted destructions through simulation tests. The failure tolerance and attack vulnerability were measured by global network performance and the size of giant component. Quantitative results in Section 4.3 showed that the BSS was a close topological analogy to the BA network, i.e., maintaining structural stability to random

Table 4
The subtle difference in *GNE* and *RSMCS* derived from different parameters when simulating the malicious attacks using the *Imp*. The initial values for all parameters are identical, i.e., *GNE* = 0.1 and *RSMCS* = 1.0.

Parameters		Global efficiency		S-Giant component	
n_1	n_2	Minimum	Mean	Minimum	Mean
0.1	0.9	0.0278	0.064	0.3780	0.7365
0.2	0.8	0.0254	0.061	0.3402	0.7265
0.3	0.7	0.0231	0.059	0.3234	0.7165
0.4	0.6	0.0227	0.056	0.2879	0.6978
0.5	0.5	0.0221	0.052	0.2581	0.6663
0.6	**0.4**	**0.0216**	**0.050**	**0.2581**	**0.6633**
0.7	0.3	0.0229	0.051	0.2783	0.6787
0.8	0.2	0.0246	0.054	0.2854	0.6924
0.9	0.1	0.0257	0.059	0.3257	0.7198

faults while being vulnerable to malicious destructions. A question we naturally ask is: how can we improve the resilience of a subway system? General solutions seem to build more interchange stations. However, the positions and the number of interchange stations deserve to be further discussed. The BSS, for instance, was designed as ring-shaped rail transit that concentrically surrounds the city. It is a distinctive transportation pattern existing in Chinese major cities such as Shanghai and Guangzhou, which is determined by their development pattern. These ring-shaped transportations can alleviate the population pressure and ensure a largest coverage. However, the local connectivity in this transportation structure seems to be weak, which merely relies on a few hub stations concentrating on urban centers. When those hubs are confronted with MAs, not only local components but global also system is considerably destroyed, which could be validated by the spatial analyses results in Section 4.4.

Consequently, several measures should be taken in order to strengthen the structural robustness of a subway network: (i) to enhance spatial correlation among various stations. This kind of correlation could be comprehensively considered from several aspects, such as economy and society in accordance with specific context; (ii) to strengthen the local connectivity while maintaining global load equilibrium. This idea could be illustrated by a checkerboard layout of Tokyo Subway, where hub stations are distributed evenly throughout whole system and load on each line is approximately equal. These span-uniform interchange stations enable the subway to provide sufficient alternatives under attack. Moreover, the well-distributed lines ensure that a local disruption cannot cause a severe damage to the global structure; (iii) to increase the spans among different transfer sites in an interchange station (Section 3.3). Transfer site usually means the entry or exit of a station. The increase of their spans would reduce the mutual influence inside a station when random faults occur to some of these sites, which is able to alleviate the population burden of a transfer site as well. Besides, according to our results and previous research

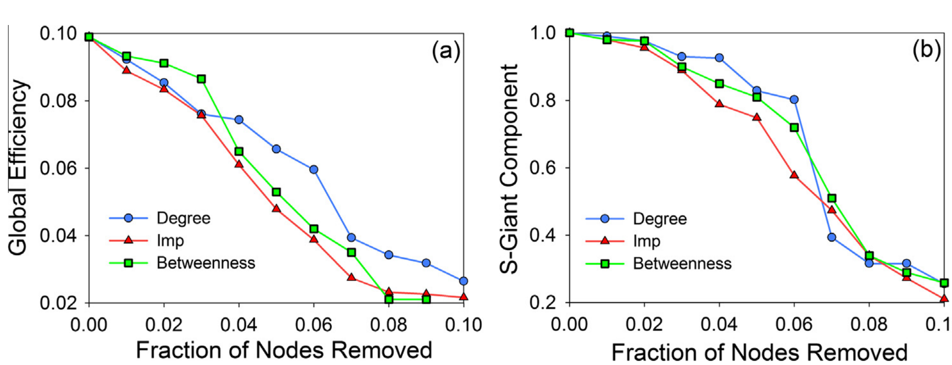

Fig. 11. Evaluation of the effectiveness of the *Imp*, node degree and betweenness through variations in the network's (a) *GNE*, and (b) *RSMCS*.

(Strogatz, 2001), a scale-free network or its topological analogies are vulnerable to attacks. Therefore, how to modify the node degree proportion to avoid the typical distribution feature would be an important and interesting point for transportation planning.

5.4. Generality and application

The promotion of a subway network's robustness is an extremely complicated issue, and comprehensive and coordinate investigations are requisite to be carried out by relevant scientific fields. Our current study aims to investigate the underlying relationship between structure of the BSS and its robustness from the generic aspects of complex network. Thus, several operations such as capacity, flows are not considered in this study but will not affect the derived conclusion of topological features compared with relevant studies (Berche et al., 2009; Flammini et al., 2009a,b; Lee et al., 2008). Although we only take the BSS as an example, this investigation and the practice are possible to be built into the safety management of other large-scale subway systems, such as London Subway and New York Subway, due to their similar topological characteristics with the BSS (Angeloudis and Fisk, 2006). We believe our current results may contribute to a baseline and several basic indexes for further research, which can be incorporated into more complex network such as bus transportation, shipping and aviation transportation.

6. Conclusions

To summarize, both complex network theory and GIS techniques are applied in this study to explore the failure tolerance and attack vulnerability of a rail transit, aiming to find reasonable ways to improve the robustness of rail transit. The BSS, a typical resource of subway network research, is taken as an example to conduct an in-depth study to examine how a subway system responds to a RF and a MA.

(1) Quantitative analyses on the topological properties show that the BSS possesses the typical features of a scale-free network, characterized by a relatively small characteristic path length and a degree distribution that conforms to the power-law distribution.
(2) A new evaluation indicator (*Imp*) for node importance evaluation is proposed and validated, which is applied to position hubs for rail transit networks.
(3) A rail transit system belonging to a scale-free network usually exhibits a relatively high level of fault tolerance and robustness when encountering a RF, but a relatively low degree of connection reliability when the hubs undergo a MA.

Although this work makes progress on the assessment of the robustness of the subway system and we have confidence in the results, due to the limitation of the network scale, practice in the BSS expose several insufficiencies. In our further research, ground transportation systems, corresponding study of flows, cost/benefit indices and the frequency of threat occurrence would, therefor, integrated into the current work to optimize a risk assessment model and safety management strategy.

Acknowledgements

This research is supported by the National Natural Science Foundation of China (Nos. 41171325, 41471068, 41230751, and J1103408), the Program for New Century Excellent Talents in University (NCET-12-0264), the Fundamental Research Funds for the Central Universities, the Priority Academic Program Development of the Jiangsu Higher Education Institutions (PAPD), and the National Key Project of Scientific and Technical Supporting Programs funded by the Ministry of Science & Technology of China (No. 2012BAH28B02). The anonymous reviewers and the editor of this paper are also acknowledged for their constructive comments and suggestions. Note that any errors or shortcomings in the paper are the responsibility of the authors.

Appendix A

See Table A1.

Table A1
Station information of the BSS.

ID	Name	Degree	ID	Name	Degree	ID	Name	Degree
1	GuCheng	2	101	Airport Terminal 3	2	201	HuangChun West Street	2
2	BaJiao Amusement Park	2	102	ZhiChun Road	4	202	QingYuan Road	2
3	BaBaoShan	2	103	ShaoYaoJu	4	203	ZaoYuan	2
4	YuQuan Road	2	104	Olympic Sports Center	2	204	GaoMiDian South	2
5	WuKeSong	2	105	FengTaiBeiLu	4	205	GaoMiDian North	2
6	WanShou Road	2	106	HuaXiang	2	206	XiHongMen	2
7	GongZhuFen	4	107	YiHaiHuaYuan	2	207	XinGong	2
8	Military Museum	2	108	FengTaiKeJiYuan	2	208	ShouTiNanLu	4
9	MuXiDi	2	109	GuoGongZhuang	2	209	BaiZhuiZi	2
10	NanLiShi Road	2	110	LuGouQiao	1	210	XiKe	3
11	FuXinMen	4	111	XiDaoKou	2	211	TaiPing	2
12	XiDan	4	112	WuLiDian	2	212	LiuLiQiao	4
13	Tian'Anmen West	2	113	FengTaiTiYu	2	213	Forest Park	2
14	Tian'Anmen East	2	114	XiJu	4	214	Olympic Part	2
15	JianGuoMen	4	115	LiZe Road	2	215	AnHeQiao North	1
16	ChaoYangMen	4	116	SanLuJu	2	216	GongYiXiQiao	2
17	DongSiShi	2	117	YuLinXi Road	2	217	JiaoMenXi	4
18	DongZhiMen	4	118	YouAnMen	3	218	MaJiaBao	2
19	AnDingMen	2	119	MaJiaBao	2	219	BeiJing South	3
20	GuLou Street	4	120	YongDingMen	2	220	TaoRanTing	2
21	JiShuiTan	2	121	AnLeLin Road	2	221	CaiShiKou	4
22	GuoMao	4	122	FangGu Road	2	222	LingJingHuTong	2
23	DaWang Road	2	123	FangZhuangDong Road	2	223	XiSi	2
24	LongZe	2	124	ShiLiHe	2	224	PingAnLi	2

Table A1 (*continued*)

ID	Name	Degree	ID	Name	Degree	ID	Name	Degree
25	HuiLongGuan	2	125	HongYan Road	2	225	XinJieKou	2
26	TuQiao	1	126	SongYuBei Road	2	226	DongWuYuan	2
27	LinHeLi	2	127	NanMoFang Road	2	227	XiBaLiZhuang	2
28	LiYuan	2	128	GuangQu Road	4	228	LianHuaQiao	2
29	JiuKeShu	2	129	ChaoYang Road	2	229	LiuLiQiaoBei	2
30	GuoYuan	2	130	JinTai Road	4	230	NiWa	2
31	TongZhouBei	2	131	ChaoYang Park	2	231	FengTai Road	2
32	BaLiQiao	2	132	DongSiHuan Road	2	232	FanJiaCun	2
33	GuanZhuang	2	133	LiangMaQiao Road	2	233	CaoQiao	2
34	ShuangQiao	2	134	JiangTai Road	2	234	JiaoMen East	2
35	Communication University of China	2	135	WanHongXiJie	4	235	DaHongMen	2
36	GaoBeiDian	2	136	WangJing	2	236	ShiLiuZhuang	2
37	Sihui East	2	137	GuangShunQiaoBei Street	2	237	TieJiangYin	2
38	Sihui East	2	138	WangDong	2	238	FenZhongShi	2
39	DaZhong Temple	2	136	WangJing2	2	239	PanJiaYuan	2
40	WuDaoKou	2	140	GuangShunQiao	2	240	HouHai	2
41	ShangDi	2	141	GuangShunQiaoBei	2	241	YongTaiZhuang	2
42	XierQi	3	142	LaiGuangYin	1	242	XiSanQi	2
43	HuoYin	2	143	NanSiHuan	2	243	QingHeXiaoYin	2
44	BeiYuan	2	144	XiaoHongMen	2	244	SuZhuang Street	1
45	WangJin West	4	145	YiZhuangQiao	2	245	NanGuan	2
46	GuangXiMen	2	146	YiZhuangWenHuaYuan	2	246	DongYangZhuang	2
47	LiuFang	2	147	JiuGong	2	247	University Club	2
48	PingGuo Yuan	3	148	WanYuanJie	2	248	University of science and engineering	2
49	XiZhiMen	5	149	RongJingDongJie	2	249	GuangYang	2
50	SongJiaZhuang	2	150	RongChangDong Road	2	250	ChangYangXi	2
51	PuHuangYu	4	151	TongJiNan Road	2	251	ChangYangZhen	2
52	TianTan East	2	152	JingHai Road	2	252	DaoTian	2
53	CiQiKou	4	153	CiQu	2	253	Universal Park	2
54	DongSi	4	154	YiZhuang	1	254	NanZhao Road	1
55	DengShiKou	2	155	CiQu South	2	255	HanYuanZi	2
56	ZhangZiZhong Road	2	156	WanZi	2	256	FengTai	2
57	BeiXinQiao	2	157	GuangAnMen	2	257	CaiHuYin	2
58	YongHeGong	4	158	DaGuanYin	2	258	DianZiCheng	2
59	HePingXiQiao	2	159	HuFangQiao	2	259	SunHeZhan	2
60	DaTunDong Road	2	160	ZhuShiKou	2	260	XinGuoZhan	2
61	BeiYuanRoad	2	161	XinFu Street	2	261	XinGuoZhan North	2
62	LiShuiQiao South	2	162	XiZhaoShi	2	262	HouShaYu	2
63	TianTongYuan South	2	163	GuangQuMen East	2	263	ShunXiLu	2
64	TianTongYuan North	1	164	BaiZiWan	2	264	FuQianJie	2
65	CheGongZhuang	4	165	HuaGongErChang	2	265	NanFaXin	2
66	FuChengMen	2	166	ZiNanJiaYuan	2	266	ChaoBaiHe East	1
67	BeiTuCheng	4	167	HuanLeGu	2	267	DongXiaoYin	1
68	AnZhenMen	2	168	DaiTou	2	268	BeiGuanHuanDao	2
69	SanYuanQiao	2	169	JiaoHuaChang	1	269	WuZiXueYuan	2
70	LiangMaQiao	2	170	BoLiErChang	2	270	MeiShuGuan	2
71	TuanJie Lake	2	171	YuDaiHe Street	2	271	ZhanLan Road	2
72	HuJiaLou	4	172	HaoJiaFu	2	272	Tian Chun Road	2
73	JinTai West	2	173	DongBuXinCheng	2	273	XiHuangChun	2
74	ShuangJing	4	174	XinHua Street	2	274	JinAnQiao	3
75	JingSong	2	175	CaoFang	2	275	SiDaoQiao	3
76	TianTongYuan	2	176	ChangYin	2	276	ShiLong Road	2
77	LiShuiQiao	4	177	HuangQu	2	277	ShangAnChun	2
78	HePingLiBeiJie	2	178	QingNian Road	2	278	KuangWuJu	2
79	HuiXinXiJieNanKou	4	179	DaLianPo	2	279	XiaoYuan	2
80	HuiXinXiJieBeiKou	2	180	XingHuoLu	2	280	ShiMenYin	1
81	LiuJiaYao	2	181	DongDaQiao	2	281	SanJiaDian	3
82	ChangChunJie	2	182	LongFuShi	3	282	MenTouGou	1
83	XuanWuMen	4	183	DiAnMen	4	283	NiuJie	2
84	HePingMen	2	184	HouHaiXi	2	284	ShuangQing Road	3
85	QianMen	2	185	HuaYuanQiao	2	285	LiuDaoKou	2
86	CongWenMen	4	186	LingLongGongYuan	4	286	BeiShaTan	2
87	BeiJing	2	187	HuoQiYin	2	287	AnHuiBeiLi	2
88	YongAnLi	2	188	ChangChunJie	2	288	XiaoYin North	2
89	WangFuJing	2	189	CheDaoGou	2	289	DaJiaoTing	2
90	DongDan	4	190	National Liabrary	3	290	BanBiDian	3
91	BaGou	2	191	WeiGongCun	2	291	ShaHe	2
92	SuZhouJie	2	192	RenMinDaXue	2	292	ShaHe North	2
93	HaiDianHuangZhuang	4	193	ZhongGuanCun	2	293	ChangPing	2
94	ZhiChunLi	2	194	PeKing University	3			
95	XiTuCheng	2	195	YuanMingYuan	3			
96	JianDeMen	2	196	XiYuan	2			
97	MuDanYuan	2	197	BeiGongMen	2			
98	TaiYangGong	2	198	HuiLongGuanDong Street	2			
99	Agricultural Exhibition Center	2	199	YiHeZhuang	2			
100	Airport Terminal 1/2	1	200	HuangChun Street	2			

References

Abbasi, A., Hossain, L., Leydesdorff, L., 2012. Betweenness centrality as a driver of preferential attachment in the evolution of research collaboration networks. J. Inform. 6, 403–412.

Albert, R., Barabási, A.-L., 2002. Statistical mechanics of complex networks. Rev. Mod. Phys. 74, 47.

Albert, R., Jeong, H., Barabási, A.-L., 2000. Error and attack tolerance of complex networks. Nature 406, 378–382.

Angeloudis, P., Fisk, D., 2006. Large subway systems as complex networks. Physica A 367, 553–558.

Bajcar, T., Cimerman, F., Širok, B., 2014. Model for quantitative risk assessment on naturally ventilated metering-regulation stations for natural gas. Saf. Sci. 64, 50–59.

Barthélemy, M., 2004. Betweenness centrality in large complex networks. Europ. Phys. J. B – Condens. Matter Complex Syst. 38, 163–168.

Benton, D.C., Fernández Fernández, M., 2013. Social network analysis: a tool for the identification of next generation trainers. Collegian.

Berche, B., von Ferber, C., Holovatch, T., Holovatch, Y., 2009. Resilience of public transport networks against attacks. Europ. Phys. J. B 71, 125–137.

Bernardi, S., Flammini, F., Marrone, S., Merseguer, J., Papa, C., Vittorini, V., 2011. Model-driven availability evaluation of railway control systems. In: Flammini, F., Bologna, S., Vittorini, V. (Eds.), Computer Safety, Reliability, and Security. Springer, Berlin, Heidelberg, pp. 15–28.

Brandes, U., 2008. On variants of shortest-path betweenness centrality and their generic computation. Soc. Network 30, 136–145.

Bruyelle, J.-L., O'Neill, C., El-Koursi, E.-M., Hamelin, F., Sartori, N., Khoudour, L., 2014. Improving the resilience of metro vehicle and passengers for an effective emergency response to terrorist attacks. Saf. Sci. 62, 37–45.

Clauset, A., Shalizi, C.R., Newman, M.E., 2009. Power-law distributions in empirical data. SIAM Rev. 51, 661–703.

Cliff, A.D., Ord, J.K., 1981. Spatial Processes: Models and Applications. Pion, London.

Crucitti, P., Latora, V., Marchiori, M., Rapisarda, A., 2003. Efficiency of scale-free networks: error and attack tolerance. Physica A 320, 622–642.

Derrible, S., Kennedy, C., 2010. The complexity and robustness of metro networks. Physica A 389, 3678–3691.

Ding, L., Zhang, L., Wu, X., Skibniewski, M.J., Qunzhou, Y., 2014. Safety management in tunnel construction: case study of Wuhan metro construction in China. Saf. Sci. 62, 8–15.

Flammini, F., Gaglione, A., Mazzocca, N., Pragliola, C., 2009a. Quantitative security risk assessment and management for railway transportation infrastructures. In: Setola, R., Geretshuber, S. (Eds.), Critical Information Infrastructure Security. Springer, Berlin, Heidelberg, pp. 180–189.

Flammini, F., Vittorini, V., Mazzocca, N., Pragliola, C., 2009b. A study on multiformalism modeling of critical infrastructures. In: Setola, R., Geretshuber, S. (Eds.), Critical Information Infrastructure Security. Springer, Berlin, Heidelberg, pp. 336–343.

Ghedini, C.G., Ribeiro, C.H., 2011. Rethinking failure and attack tolerance assessment in complex networks. Physica A 390, 4684–4691.

Glickman, T.S., Erkut, E., 2007. Assessment of hazardous material risks for rail yard safety. Saf. Sci. 45, 813–822.

Kim, J., Wilhelm, T., 2008. What is a complex graph? Physica A 387, 2637–2652.

Kyriakidis, M., Hirsch, R., Majumdar, A., 2012. Metro railway safety: an analysis of accident precursors. Saf. Sci. 50, 1535–1548.

Latora, V., Marchiori, M., 2002. Is the Boston subway a small-world network? Physica A 314, 109–113.

Lee, K., Jung, W.-S., Park, J.S., Choi, M.Y., 2008. Statistical analysis of the Metropolitan Seoul Subway System: network structure and passenger flows. Physica A 387, 6231–6234.

Lu, Y., Li, Q., Xiao, W., 2013. Case-based reasoning for automated safety risk analysis on subway operation: case representation and retrieval. Saf. Sci. 57, 75–81.

Moran, P.A.P., 1950. Notes on continuous stochastic phenomena. Biometrika 37, 17–23.

Murray, A.T., Matisziw, T.C., Grubesic, T.H., 2008. A methodological overview of network vulnerability analysis. Growth Change 39, 573–592.

Nawrath, C., 2006. Unraveling the complex network of cuticular structure and function. Curr. Opin. Plant Biol. 9, 281–287.

Newman, M.E., Strogatz, S.H., Watts, D.J., 2001. Random graphs with arbitrary degree distributions and their applications. Phys. Rev. E 64, 026118.

Queiros-Conde, D., 2003. A Diffusion Equation to Describe Scale – and Time – Dependent Dimensions of Turbulent Interfaces.

Queiros-Conde, D., Bonjour, J., Wechsatol, W., Bejan, A., 2007. Parabolic scaling of tree-shaped constructal network. Physica A 384, 719–724.

Sen, S., Baudry, B., Mottu, J.M., 2008. On Combining Multi-formalism Knowledge to Select Models for Model Transformation Testing, Software Testing, Verification, and Validation, 2008 1st International Conference on, pp. 328–337.

Si, H., Ji, H., Zeng, X., 2012. Quantitative risk assessment model of hazardous chemicals leakage and application. Saf. Sci. 50, 1452–1461.

Silverman, B.W., 1986. Density Estimation for Statistics and Data Analysis. CRC Press.

Sparrow, M.K., 1991. The application of network analysis to criminal intelligence: an assessment of the prospects. Soc. Network 13, 251–274.

Strogatz, S.H., 2001. Exploring complex networks. Nature 410, 268–276.

Tarjan, R., 1972. Depth-first search and linear graph algorithms. SIAM J. Comput. 1, 146–160.

van der Vlies, V., van der Heijden, R., 2013. Urban planning and rail transport risks: coping with deadlocks in Dutch urban development projects. Saf. Sci. 57, 1–13.

Vernez, D., Vuille, F., 2009. Method to assess and optimise dependability of complex macro-systems: application to a railway signalling system. Saf. Sci. 47, 382–394.

Wang, J., 2013. Robustness of complex networks with the local protection strategy against cascading failures. Saf. Sci. 53, 219–225.

Wang, J., Fang, W., 2014. A structured method for the traffic dispatcher error behavior analysis in metro accident investigation. Saf. Sci. 70, 339–347.

Wang, J., Mo, H., Wang, F., Jin, F., 2011. Exploring the network structure and nodal centrality of China's air transport network: a complex network approach. J. Transp. Geogr. 19, 712–721.

Wang, H., Huang, J., Xu, X., Xiao, Y., 2014. Damage attack on complex networks. Physica A 408, 134–148.

Wu, Z.-X., Peng, G., Wang, W.-X., Chan, S., Wong, E.W.-M., 2008. Cascading failure spreading on weighted heterogeneous networks. J. Stat. Mech: Theory Exp. 2008, P05013.

Xu, Z., Sui, D.Z., 2007. Small-world characteristics on transportation networks: a perspective from network autocorrelation. J. Geogr. Syst. 9, 189–205.

Zhang, J., Xu, X., Hong, L., Wang, S., Fei, Q., 2012. Attack vulnerability of self-organizing networks. Saf. Sci. 50, 443–447.

Zhang, M., Kecojevic, V., Komljenovic, D., 2014. Investigation of haul truck-related fatal accidents in surface mining using fault tree analysis. Saf. Sci. 65, 106–117.

Zhao, L., Wang, X., Qian, Y., 2012. Analysis of factors that influence hazardous material transportation accidents based on Bayesian networks: a case study in China. Saf. Sci. 50, 1049–1055.

Zhong, M., Shi, C., Fu, T., He, L., Shi, J., 2010. Study in performance analysis of China Urban Emergency Response System based on Petri net. Saf. Sci. 48, 755–762.

Zhou, Z., Irizarry, J., Li, Q., 2014. Using network theory to explore the complexit of subway construction accident network (SCAN) for promoting safety management. Saf. Sci. 64, 127–136.